

Accepted Manuscript

Ni(II), Pd(II) and Pt(II) complexes of (1*H*-1,2,4-triazole-3-ylimino)methyl]naphthalene -2-ol. Structural, spectroscopic, biological, cytotoxicity, antioxidant and DNA binding

M. Gaber, H.A. El-Ghamry, S.K. Fathalla

PII: S1386-1425(14)01837-X

DOI: <http://dx.doi.org/10.1016/j.saa.2014.12.057>

Reference: SAA 13107

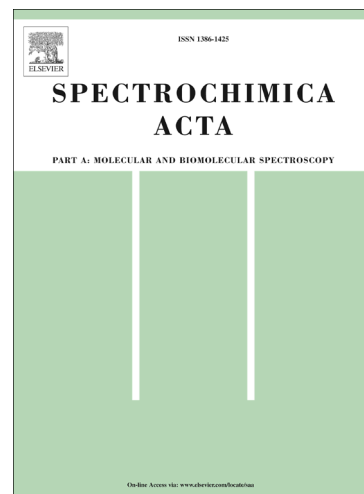
To appear in: *Spectrochimica Acta Part A: Molecular and Biomolecular Spectroscopy*

Received Date: 15 October 2014

Accepted Date: 17 December 2014

Please cite this article as: M. Gaber, H.A. El-Ghamry, S.K. Fathalla, Ni(II), Pd(II) and Pt(II) complexes of (1*H*-1,2,4-triazole-3-ylimino)methyl]naphthalene -2-ol. Structural, spectroscopic, biological, cytotoxicity, antioxidant and DNA binding, *Spectrochimica Acta Part A: Molecular and Biomolecular Spectroscopy* (2014), doi: <http://dx.doi.org/10.1016/j.saa.2014.12.057>

This is a PDF file of an unedited manuscript that has been accepted for publication. As a service to our customers we are providing this early version of the manuscript. The manuscript will undergo copyediting, typesetting, and review of the resulting proof before it is published in its final form. Please note that during the production process errors may be discovered which could affect the content, and all legal disclaimers that apply to the journal pertain.



Ni(II), Pd(II) and Pt(II) complexes of (1*H*-1,2,4-triazole-3-ylimino)methyl]naphthalene-2-ol. Structural, spectroscopic, biological, cytotoxicity, antioxidant and DNA binding.

M. Gaber ¹, H.A. El-Ghamry ^{1,2*}, S.K. Fathalla ¹

¹ Chemistry Department, Faculty of Science, Tanta University, Tanta, Egypt

² Department of Chemistry, Faculty of Applied Science, Umm Al-Qura University, Makkah, Kingdom of Saudi Arabia

Abstract

Metal complexes of the general formula $[ML(H_2O)Cl]_nH_2O$; $n=1$ for $M=Ni$ and Pt and $n=2$ for $M=Pd$, $L=$ Schiff base (HL) derived from the condensation of 3-amino-1,2,4-triazole and 2-hydroxy-1-naphthaldehyde, were prepared. The synthesized ligand and its metal complexes were characterized on the basis of elemental analyses, spectral and magnetic studies as well as thermal analysis. The IR spectra revealed that the ligand is coordinated to the metal ions in bidentate manner via the N-atom of the azomethine group and the phenolic OH group. Square planar geometry was proposed for Pd(II) and Pt(II) complexes and tetrahedral for Ni(II) complex. The ligand and its metal complexes were screened against the sensitive organisms *Escherichia coli* as Gram-negative bacteria, *Staphylococcus aureus* as Gram-positive bacteria, *Aspergillus flavus* and *Candida albicans* as fungi. Moreover, the anticancer activity of the ligand and its metal complexes was evaluated in liver carcinoma (HEPG2) cell line. The results obtained indicated that the Schiff base ligand is more effective than its metal complexes towards the tested cell line. Ni(II), Pd(II) and Pt(II) complexes as well as the free Schiff base ligand were tested for their antioxidant activities. The DNA-binding properties of the studied complexes have been investigated by electronic absorption and viscosity measurements.

Keywords: Ni(II), Pd(II), Pt(II) complexes, DNA binding, Antioxidant activity, Cytotoxicity, Antimicrobial.

* Corresponding author e.mail: helghamrymo@yahoo.co

1. Introduction

The chemistry of Schiff base ligands and their metal complexes have attracted a lot of interest due to their facile synthesis and wide range of applications. These compounds play an important role in the development of coordination chemistry related to catalysis, organic synthesis [1,2], antitumor, antimicrobial and cytotoxic activity[3-7.] Schiff bases derived from 1,2,4-triazoles and their metal complexes are biologically active having antiproliferative [8], antibacterial and antifungal activity[9-17], antitumor [18] and anticancer [19]. DNA is an important drug target and it regulates many biochemical processes that occur in the cellular system. Small metal complexes that undergo hydrolytic DNA cleavage are useful in genetic engineering molecular biotechnology and robust anticancer drug design [20]. Recently, there has been a great interest on the binding of metal complexes with DNA [21-27] because it may provide important information for new cancer therapeutic agents and potential probes of DNA structure and conformation. Pd(II) and Pt(II) complexes have attracted considerable attention in recent years because of their promising antibacterial and antitumor activity [28-39] In the view of the above and our ongoing interest in the synthesis and biological properties of various transition metal complexes [13, 40-42], we report herein the synthesis of the titled Schiff base and its Ni(II), Pd(II) and Pt(II) complexes. The synthesized ligand and its metal complexes were characterized by different techniques like elemental analyses, spectral studies, TGA, magnetic and conductance measurements. The biological screening, antioxidant and anticancer activities of the Schiff base ligand and its metal complexes are also described here.

2. Experimental

2.1. Chemicals

All compounds used in the present study were of pure grade available from BDH, Aldrich or Sigma. The solvents used for the spectral study were spectroscopic grade from Aldrich.

2.2. Preparation of Schiff-base ligand (SB)

The Schiff base ligand (**Fig. 1**) was prepared by the condensation of 3-amino-1,2,4-triazole with 2-hydroxy-1-naphthaldehyde, in 1:1 mole ratio in hot methanol as a solvent and refluxed for 8 h according to the recommended method.[13,42] It was achieved by refluxing 0.01 mol (1.72 g) of 2-hydroxy-1-naphthaldehyde with 0.01 mol (0.84 g) of 3-amino-1,2,4-

triazole in methanol (100 mL) as a solvent. The condensation product separated on cooling was filtered off, washed several times with methanol till constant melting point and finally dried in a vacuum desiccator over anhydrous calcium chloride.

2.3. Preparation of the solid metal complexes

To a hot solution (1 mmol) of Schiff base ligand in (50 ml) methanol, a hot solution of corresponding metal chlorides [$\text{NiCl}_2 \cdot 6\text{H}_2\text{O}$, K_2PdCl_4 and K_2PtCl_4] (1 mmol, in 50 ml methanol) were added slowly by the molar ratio 1:1 (L:M) in the presence of few drops of triethyl amine as basic medium.. The resulting mixtures were stirred and refluxed on a hot plate for 10 hours and then concentrated to a small volume; the solid complexes, which separated out on hot, were filtered off, washed several times with methanol and finally deride in a vacuum desiccator over anhydrous CaCl_2 .

2.4. Physical measurements

The elemental microanalyses of the prepared compounds were performed in the microanalytical center, Cairo University using Perkin-Elmer 2400 CHN Elemental analyzer. The Infrared spectra were recorded on a Perkin-Elmer 1430 IR spectrophotometer within the range $4000\text{-}200\text{ cm}^{-1}$ as KBr discs. The ^1H NMR spectra were carried out using a Varian Mercury Oxford NMR 300 Hz spectrophotometer after dissolving the samples in DMSO d-6 using tetramethylsilane as internal standard. The electronic absorption spectra were recorded using a Shimadzu Uv-Vis 240 spectrophotometer. The electron impact mass spectra of the complexes were recorded at 70 eV. The magnetic susceptibility of the solid complexes was carried out at room temperature by the Gouy's technique for magnetic susceptibility instrument. The thermogravimetric analysis (TGA) of the solid complexes were performed using the Schimadzu TG-50 thermogravimetric analyzer with heating rate $10^\circ\text{C}/\text{min}$ under nitrogen atmosphere, in the range $25\text{-}800^\circ\text{C}$.

2.5. DNA binding studies

The experiments were carried out in Tris-HCl buffer (5.0 mM of tris (hydroxymethyl)-aminomethane and 50 mM NaCl) at pH 7.2. Tris-HCl buffer was prepared using deionized and triple distilled water. Solutions of DNA in Tris-HCl gave a ratio of UV absorbance at 260

and 280 nm (A_{260}/A_{280}) of 1.8–1.9, indicating that the DNA was sufficiently free from protein [43, 44]. The stock solution of DNA was prepared by dissolving DNA in Tris–HCl buffer. Concentrated stock solutions of metal complexes were prepared by dissolving in DMF and diluted suitably to required concentration. The spectroscopic titrations were carried out by adding increasing amounts of DNA to a solution of the complex at a fixed concentration. When measuring the absorption spectra, an equal amount of DNA was added to both the complex solutions and the reference solution to eliminate the absorbance of DNA itself. The intrinsic binding constant K_b was determined from the plot of $[\text{DNA}]/(\epsilon_a - \epsilon_f)$ versus $[\text{DNA}]$, according to the following Eq.

$$[\text{DNA}]/(\epsilon_a - \epsilon_f) = [\text{DNA}]/(\epsilon_b - \epsilon_f) + 1/ [K_b(\epsilon_b - \epsilon_f)]$$

where $[\text{DNA}]$ is the concentration of DNA in base pairs, the apparent absorption coefficients ϵ_a , ϵ_f and ϵ_b correspond to $A_{\text{obs}}/[\text{complex}]$, extinction coefficient for the free complex and the extinction coefficient of the complex in the totally bound form, respectively. The data were fitted to the above equation and graph was obtained with a slope equal to $1/(\epsilon_b - \epsilon_f)$ and intercept equal to $1/[K(\epsilon_b - \epsilon_f)]$. Hence K_b was obtained from the ratio of the intercept to the slope [45].

Viscosities of CT-DNA at different complex concentrations in buffer solution were measured using Ubbelodhe viscometer at the temperature of 30 ± 0.1 °C in a thermostatic water-bath. The DNA concentration was fixed, but the complex concentration was increased each time. The average flow time was obtained after three times measurement for a sample with a digital stopwatch. Data were presented as $(\eta/\eta_0)^{1/3}$ vs. mole ratio of $[\text{complex}]/[\text{DNA}]$, where η and η_0 are the specific viscosity of DNA in presence and in absence of the complex, respectively. The values of η and η_0 were calculated by using the equation:

$$\eta = (t-t_0)/t_0$$

where "t" is the observed flow time of a solution containing DNA and the complexes and "t₀" is the flow time of the DNA solution alone. The relative viscosities for DNA were calculated from the relation (η/η_0) [46].

2.6. Biological activity

Antimicrobial activity of the synthesized compounds was determined using disc-agar diffusion method [47] against the sensitive organisms *Escherichia coli* as Gram-negative bacteria, *Staphylococcus aureus* as Gram-positive bacteria, *Aspergillus flavus* and *Candida albicans* as fungi. Standard discs of Tetracycline (Antibacterial agent), Amphotericin B (Antifungal agent) served as positive controls for antimicrobial activity but filter discs impregnated with 10 μ l of solvent (DMSO) were used as a negative control. Briefly, 100 μ l of the test bacteria/fungi were grown in 10 ml of fresh media until they reached a count of approximately 10^8 cells/ml for bacteria or 10^5 cells/ml for fungi [48]. 100 μ l of microbial suspension was spread onto agar plates corresponding to the broth in which they were maintained. Plates incubated with filamentous fungi as *Aspergillus flavus* at 25 °C for 48 hours; Gram (+) bacteria as *Staphylococcus aureus* and Gram (-) bacteria as *Escherichia coli* they were incubated at 35-37 °C for 24-48 hours and yeast as *Candida albicans* incubated at 30 °C for 24-48 hours and, then the diameters of the inhibition zones were measured in millimeters [47]. Blank paper disks (Schleicher & Schuell, Spain) with a diameter of 8.0 mm were impregnated 10 μ l of tested concentration of the stock solutions. When a filter paper disc impregnated with a tested chemical is placed on agar the chemical will diffuse from the disc into the agar. This diffusion will place the chemical in the agar only around the disc. Inhibition of the organisms which evidenced by clear zone surround each disk was measured and used to calculate mean of inhibition zones.

2.7. Measurement of Potential cytotoxicity by SRB assay

Liver carcinoma (HEPG2) Human cancer cell line was used for in vitro screening experiments. This cell line was obtained frozen in liquid nitrogen (-180 °C) from the American Type Culture Collection. The tumor cell line was maintained in the National Cancer Institute, Cairo, Egypt, by serial sub-culturing. Potential cytotoxicity of the compounds was tested using Skehan et al. method [49]. Cell was plated in 96-multiwell plate (10^4 cells/well) for 24 hrs before treatment with the compound to allow attachment of cell to the wall of the plate. Different concentrations of the compounds under study (0, 5, 12.5, 25 and 50 μ g/ml) were added to the cell monolayer triplicate wells prepared for each individual dose. The monolayer cell was incubated with the compounds for 48 hrs at 37 °C and in atmosphere of 5% CO₂. After 48 hrs, Cell was fixed, washed and stained with the protein-binding dye Sulfo-Rhodamine-B (SRB)

[50]. Excess stain was washed with acetic acid and attached stain was recovered with Tris EDTA buffer. Color intensity was measured in an ELISA reader. The relation between surviving fraction and drug concentration is plotted to get the survival curve of each tumor cell line after the specified compound. Potential cytotoxicity of the compounds was measured in (Pharmacology Unit, Cancer Biology Department, National Cancer Institute, Cairo University). Doxorubicin was used as standard cytotoxins.

2.8. DPPH radical scavenging

The antioxidant activity of the investigated compounds and the standard ascorbic acid were assessed on the basis of the radical scavenging effect of the stable DPPH (1,1-diphenyl-2-picryl hydrazyl) free radical. The radical scavenging effects of antioxidants on DPPH are due to their hydrogen donating ability which causes an absorbance drop at 517 nm.

In the DPPH radical scavenging, antioxidants react with the DPPH radical, which is a stable free radical and exists naturally in deep violet color, to turn into a yellow colored (diphenyl--picryl hydrazine). The degree of discoloration indicates the radical scavenging potential of the antioxidant [51].

1 µg of the studied samples and ascorbic acid (reference compound) were dissolved in DMSO (1 ml). 250 µl of each solution was added to 1 ml DPPH/DMSO solution (6 mg/50 ml) and the total volume was adjusted to 3 ml with DMSO. After vortexing the mixture was incubated for 30 min at room temperature. Absorbance was measured at 517 nm. Absorbance of blank sample containing the same amount of DMSO and DPPH solution was prepared and measured as well. The experiment was carried out in triplicate. The scavenging potential was compared with a solvent control (0% radical scavenging) and ascorbic acid. Radical scavenging activity was calculated by the following formula:

$$\% \text{ Reduction of absorbance} = [(AB - AA)/AB] \times 100$$

Where: AB – absorbance of blank sample; AA – absorbance of tested sample

3. Results and discussion

3.1. The elemental analysis and molar conductance results

On the basis of elemental analysis the complexes were assigned the composition shown in **Table 1**. The results obtained are in good agreement with those calculated for the suggested molecular formulae. The molar conductance values listed in **Table 1** revealed that the

complexes are non-electrolytes in DMF [52]. Thus, the general formulae of the complexes is $[\text{ML}(\text{H}_2\text{O}) \text{Cl}] n\text{H}_2\text{O}$, where $n=1$ for $M= \text{Pt}$ or Ni ; $n=2$ for $M= \text{Pd}$.

3.2. Infrared spectra

The IR spectra of the metal complexes are compared with that of the free Schiff base ligand in order to determine the coordination sites that may be involved in chelation, **Table 2**. The IR spectrum of the free ligand showed strong bands at 1614 cm^{-1} and 1575 cm^{-1} due to $\nu_{\text{C=N}}$ of triazole moiety and azomethine group, respectively [53]. The ν (C=N) of the free azomethine group is shifted to lower values ($1538\text{-}1553 \text{ cm}^{-1}$) indicating its involvement in the coordination sphere [54]. The involvement of the deprotonated phenolic OH group in complex formation is confirmed by the blue shift of the ν (C-O) stretching band ($1280\text{-}1307 \text{ cm}^{-1}$) in complex formation [55]. IR spectra of all complexes showed broad bands at ($3378\text{-}3413$) cm^{-1} which can be assigned to ν_{OH} of lattice water molecules associated with complexes [56]. The participation of oxygen and nitrogen atoms in coordination with the metal ion is further supported by the appearance of new bands within the range ($556\text{-}611$), ($426\text{-}535$) cm^{-1} due to $\nu_{\text{M-O}}$ and $\nu_{\text{M-N}}$, respectively.

3.3. ^1H NMR spectra

The ^1H NMR spectrum of the Schiff base ligand showed singlet signals at 10.08 and 8.44 ppm due to phenolic (-OH) and azomethine (-CH=N-) protons, respectively. The signal due to the phenolic proton is absent, while the signal due to the azomethine proton is shifted to 8.93 and 8.95 ppm in the spectra of Pd(II) and Pt(II) complexes, respectively. This observation supported the involvement of the OH and azomethine nitrogen in complex formation, **Table 3**.

3.4. EI- Mass spectra

The EI-mass spectra of Schiff base complexes showed the molecular ion peaks at (m/z) 366, 433 and 503 for Ni(II), Pd(II) and Pt(II) complexes, respectively, which agree with the formula weights of the complexes. The fragmentation patterns of the complexes are illustrated in **Schemes (S1- S3)**.

3.5. Electronic spectra and magnetic moments

The magnetic moment value of Ni(II) complex is 3.35 B.M corresponding to two unpaired electrons which is consistent with the tetrahedral structure of the complex [57]. All

the Pd(II) and Pt(II) complexes exhibit diamagnetic character confirming the square-planar geometry. The Nujol mull spectrum of Ni(II) complex (1) showed broad d–d transition band at 23419 cm^{-1} attributed to ${}^3T_1 \rightarrow {}^3T_1(p)$ transition indicating tetrahedral geometry [58]. The electronic spectrum of Pt(II) complex exhibited a low energy spin allowed band at 23364 cm^{-1} corresponding to the transition $b_{2g}(d_{xy}) - d_{1g}(d_{x^2-y^2})$ i.e. ${}^1A_{1g} \rightarrow {}^1A_{2g}(v_1)$ comparable to the transition assigned by Jorgensen [59] for $[\text{PtCl}_4]^{2-}$ (21500 cm^{-1}). The bands at 28986 cm^{-1} and 28818 cm^{-1} for Pd(II) and Pt(II) complexes, respectively, are assignable to a combination of $eg(d_{yz}, d_{zx}) - b_{1g}(d_{x^2-y^2})$ i.e. ${}^1A_{1g} \rightarrow {}^1E_g(v_3)$ and MLCT indicating a square planar geometry [60].

3.6. Thermogravimetric analysis (TGA) of the complexes

The thermal behavior of the metal complexes was studied using TG technique. The stages of decomposition, temperature range, mass loss percentages as well as decomposition products are given in **Table S1**.

The thermal decomposition of Ni(II) complex takes place in five steps, the first step of decomposition within the temperature range $38\text{--}136\text{ }^\circ\text{C}$ with mass loss 9.80% (calc. 9.98%) corresponded to elimination of two water molecules. The second step at $136\text{--}410\text{ }^\circ\text{C}$ with mass loss 27.23% (calc. 28.16%) can be assigned to elimination of (Cl and triazole ring). The third step at $410\text{--}467\text{ }^\circ\text{C}$ with mass loss 17.42% (calc. 17.96%) represents the loss of $(\text{C}_4\text{H}_4\text{N})$. The fourth step at $467\text{--}533\text{ }^\circ\text{C}$ with mass loss 13.79% (calc. 13.33%) correspond to loss of (C_4H) . The final step at $533\text{--}660\text{ }^\circ\text{C}$ with mass loss 11.25% (calc. 10.34%) represents the further dissociation of the ligand with the formation of NiO as a final product. The thermogram of Pd(II) complex comprises three steps. The first step at $45\text{--}100\text{ }^\circ\text{C}$ with mass loss 8.65% (calc. 8.32%) correspond to elimination of 2 hydrated water molecules. The second step at $100\text{--}337\text{ }^\circ\text{C}$ with mass loss 28.33% (calc. 28.09%) can be assigned to the loss of coordinated water molecule, Cl^- anions and triazole ring. The third step at $337\text{--}458\text{ }^\circ\text{C}$ with mass loss 27.44% (calc. 27.05%) represents the decomposition of the organic ligand with the formation of $\text{PdO} + 3\text{C}$ as a final product. The thermal decomposition of Pt(II) complex comprises two steps. The first step at $40\text{--}103\text{ }^\circ\text{C}$ with mass loss 3.21% (cal. 3.57%) correspond to elimination of hydrated water molecule. The second step at $103\text{--}590\text{ }^\circ\text{C}$ with mass loss 31.67% (calc. 32.08%) can be assigned to the loss of coordinated water molecule,

Cl⁻ anions and decomposition of the organic ligand with the formation of PtO + C₈H₄ as a final product.

The kinetic parameters (the order *n*, pre-exponential factor *A* and activation energy ΔE) for the thermal decomposition steps were evaluated graphically using the Coats-Redfern equation [61], Fig 2.

The thermodynamic activation parameters (ΔH), (ΔS) and (ΔG) were calculated using the relationships:

$$\Delta H = \Delta E - RT$$

$$\Delta S = R [\ln(Ah/kT) - 1]$$

$$\Delta G = \Delta H - T \Delta S$$

Where *k* is Boltzmann constant and *h* is Planck's constant.

From the results listed in Table 4:

- 1- The negative values of the activation entropies ΔS^* indicate a more ordered activated complex than the reactants and/or the reactions are slower than normal [62].
- 2- The positive values of ΔH mean that the decomposition processes are endothermic [63].
- 3- Kinetics of the thermal decomposition stages of all complexes under study obeys, in most cases, the first order kinetics.
- 4- The values of activation energies increase as the maximum temperature of decomposition increases reflecting higher stability of the formed complexes under investigation.

Based on the above results, the schematic structures of the metal complexes is shown in Fig. 3

3.7. DNA studies

To evaluate the DNA interaction properties of the synthesized compounds, the UV-Vis absorption and viscosity titration techniques were performed using CT-DNA. Absorption spectral titration experiments were performed by maintaining a constant concentration of the complex and varying concentration of CT-DNA. Hypochromism and hyperchromism are both spectral features of DNA connected with its double helix structure. Hypochromism means the DNA binding mode of the complex is electrostatic which can stabilize the DNA duplex [64]. The extent of hypochromism is commonly consistent with the strength of intercalative interaction [65]. The hyperchromism means the breakage of the secondary structure of DNA [64,66]. Complex bind to DNA through intercalation usually results in hypochromism

(decrease in absorbance) and bathchromism (red shift) because intercalative mode involves a strong stacking interaction between aromatic chromophore and the base pairs of DNA [67]. The absorption spectra of the ligand and its Ni(II), Pd(II) and Pt(II) complexes in the absence and presence of CT-DNA are shown in **Fig. 4**. The electronic absorption of the Schiff base ligand and its Pd(II) and Pt(II) complexes showed an increase in intensity with increasing the concentration of the DNA i.e upon addition of increasing amount of CT-DNA, a significant hyperchromic effect was observed. This suggested the existence of strong interaction between the Pd(II) and Pt(II) complexes and CT-DNA which is different from the classical intercalation binding. The observed hyperchromism was 21 % and 61 % for Pd(II) and Pt(II) complexes, respectively. The spectral change of the complexes C2 and C3 observed in the presence of CT-DNA can be rationalized in terms of groove binding [68]. The addition of increasing concentration of CT-DNA ($0 - 60 \times 10^{-6}$ M) to a fixed concentration of Ni(II) complex (8×10^{-5} M) resulted in the hypochromism with red shift ($\Delta\lambda = 2$ nm). The spectral characteristics suggested that Ni(II) complex interacted with CT-DNA by the intercalative binding mode because intercalation leads to hypochromism and bathochromism in absorption spectra.

The intrinsic binding constant (k_b) for Ni(II), Pd(II) and Pt(II) complexes was found to be (3.08×10^5 , 17.68×10^5 , 5.52×10^5) M^{-1} respectively, **Table S2**. From the results listed in **Table S2**, we could deduce that Ni(II), Pd(II) and Pt(II) complexes bind to DNA with high affinities and the DNA binding affinity of Pd(II) complex is stronger than Ni(II) and Pt(II) complex [69]. Non planarity of the Ni(II) complex may be the main reason for the lower k_b value of the Ni(II) complex compared to Pd(II) and Pt(II) complexes i.e the geometry of the complex affects the magnitude of binding [70]

3.8. Viscosity measurements

To further make clear the interaction between the complex and DNA, viscosity measurements were studied. A classical intercalative mode causes a significant increase in viscosity of DNA solution due to increase in overall DNA length. In contrast, complexes those bind exclusively in the DNA grooves by partial and/or non-classical intercalation under the same conditions, typically cause less pronounced (positive or negative) or no change in DNA solution viscosity [71]. The effect of increasing amount of complexes on the relative

viscosity of DNA is shown in **Fig. 5**. The gradual increase in relative viscosity was observed on addition of the metal complexes to DNA solution suggesting mainly intercalation mode of binding with the complexes [71,72] i.e. the observed increase in the relative viscosity of DNA could be as a result of a length increase of the duplex on intercalation of the complex. This phenomenon may be explained by the insertion of the compounds in between the DNA base pairs, leading to an increase in the separation of base pairs at intercalation sites and thus an increase in overall DNA length [73].

3.9. Antimicrobial activity

The synthesized Schiff base (SB) and its Ni(II), Pd(II) and Pt(II) complexes have been tested for their inhibitory effect on the growth of bacteria: *E. coli* and *S. aureus* and fungi: *A. flavus* and *C. albicans*. The antibacterial and antifungal activity values of the investigated compounds are tabulated in **Table 5**.

With regard to *A. flavus*, the results indicated that the Schiff base ligand and its complexes showed no activity. With *C. albicans*, the Schiff base ligand showed moderate activity while Ni(II), Pd(II) and Pt(II) complexes exhibited the lower activity. On the basis of inhibition zone produced against the *E. coli* and *S. aureus* bacteria (9-13 mm), all the complexes have moderate activity except Ni(II) complex with *E. coli* (9 mm) and *S. aureus* (9 mm) which has low activity. A possible explanation for the poor activity of these complexes in comparison to the Schiff base ligand may be due to their inability to chelate metals essential for the metabolism of microorganisms and/or to form hydrogen bonds with the active centers of cell structures, resulting in an interference with the normal cell cycle. It is also due to their low lipophilicity, where the penetration of the complex through the lipid membrane is decreased and hence, they cannot block or inhibit the growth of the microorganism [35]

3.10. Anticancer activity

The anticancer activity of the SB ligand and its complexes was determined in vitro on human tumor cell line (liver carcinoma HEPG2), **Fig. 6**. The IC_{50} (the concentration that inhibited in 50% of the cellular proliferation) was determined. According to Shier [74], the compounds exhibited IC_{50} activity within the range of 10-25 $\mu\text{g/ml}$ are considered weak anticancer drugs, while those of IC_{50} activity between 5 and 10 $\mu\text{g/ml}$ are moderate and compounds of activity below 5.00 $\mu\text{g/ml}$ are considered strong agents. It was found that the ligand exhibited strong antitumor activity and its Ni(II), Pd(II) and Pt(II) complexes exhibited

a weak antitumor activity according to Shier scale. The results obtained indicated that the Schiff base ligand is more effective than its complexes towards the cancer cell line. The results showed the higher toxicity of Pd(II) (19.7 $\mu\text{g/ml}$) complex than Pt(II) (19.5 $\mu\text{g/ml}$) and Ni(II) (15.5 $\mu\text{g/ml}$) complexes, **Table 6**.

3.11. Antioxidant

Hydroxyl radical is highly reactive oxygen centered radical formed from the reactions of various hydroperoxides with transition metal ions. This radical is by far the most potent and therefore the most dangerous oxygen metabolite and hence the elimination of this radical is one of the major aims of antioxidant administration [75]. It attack proteins, DNA, polysaturated fatty acid in membranes and most biological molecules [76]

Nowadays, antioxidants that exhibit DPPH radical scavenging activity are increasingly receiving attention. The model of the scavenging of the stable DPPH radical is extensively used to evaluate the antioxidant activities in less time than the other methods. The competition of the complex with DMSO for hydroxyl radicals, generated by the Fe^{3+} / ascorbic acid system expressed as the inhibition of formaldehyde production was used for the evaluation of their hydroxyl radical scavenging activity.

Ni(II), Pd(II) and Pt(II) complexes as well as the free Schiff base ligand were tested for their antioxidant activities. The radical scavenging activity of the investigated compounds was tested against (the DPPH stable free radical) the hydroxyl radical generated by Fe^{3+} / ascorbic acid system. In the present study, based on the IC₅₀ values, scavenging activities of the free Schiff base ligand and its Ni(II), Pd(II) and Pt(II) complexes are calculated. The comparison of the antioxidant activity of the SB ligand (IC₅₀ = 83.91 mg/ml) with those of the metal complexes (IC₅₀ values of Ni(II), Pd(II) and Pt(II) complexes are 73.72, 57.39 and 86.64 mg/ml, respectively) indicated that (i) Ni(II) and Pd(II) complexes possess higher scavenging activities towards the hydroxyl radical than the free ligand. (ii) Pd(II) complex showed more scavenging activity than Ni(II) and Pt(II) complexes. In general, the antioxidant activity of the SB ligand and its metal complexes was found to decrease in order of Pd(II) > Ni(II) > SB > Pt(II).

4. Conclusion

Schiff base ligand derived from condensation of 3-amino-1, 2, 4-triazole with 2-hydroxy-1-naphthaldehyde and its metal complexes with Ni(II), Pd(II) and Pt(II) have been described and characterized by the combination of the elemental analysis, ¹HNMR, IR, mass, electronic spectra, magnetic susceptibility and thermal analysis. The metals are coordinated to the nitrogen atoms of the azomethine and phenolic oxygen atom. The magnetic moment values of the complexes display diamagnetic behavior for Pd(II) and Pt(II) complexes and tetrahedral geometrical structure for Ni(II) complex. All the complexes have moderate activity towards the *E. coli* and *S. aureus* bacteria except Ni (II) complex with *E. coli* and *S. aureus* which has low activity. The Schiff base ligand and its complexes showed no activity against *A. flavus*. With *C. albicans*, the Schiff base ligand showed moderate activity while Ni(II), Pd(II) and Pt(II) complexes exhibited the lower activity. The free Schiff base ligand and its complexes show anticancer activity against HEPG2 cell. The Schiff base ligand exhibited strong antitumor activity while its Pd(II), Pt(II) and Ni(II) complexes exhibited a weak antitumor activity. The results obtained indicated that the SB ligand is more effective than their complexes towards the cancer cell line. The in vitro antioxidant of the ligand and its metal complexes were also carried out. The order of the scavenging activity of the metal complexes according to their IC50 values is Pd(II) > Ni(II) > Pt(II).

Acknowledgements

Financial support from Tanta University, Tanta, Egypt is gratefully acknowledged. The authors would like to thank Prof. Dr. T. Mostafa and Dr. Mai M. El-Keiy, Chemistry Department, Biochemistry Specialty, Faculty of Science, Tanta University, Egypt for their help with the antioxidant activity studies.

Reference

- [1] T. Rosu, E. Pahontu, M. Reka-Stefana, D. Ilies, R. Georgescu, S. Shova, A. Gulea. *Polyhedron* 31 (2012) 352-360.
- [2] R. Antony, S. David, K. Saravanan, K. Karuppasamy, S. Balakumar, *Spectrochim. Acta A*, 103 (2013) 423-430.
- [3] Z. You, D. Shi, C. Xu, Q. Zhang, H. Zhu. *Eur J Med Chem.* 43 (2008) 862-71
- [4] K. Singh, M.S. Barwa, P. Tyagi. *Eur. J. Med. Chem.* 41 (2008) 147-153.
- [5] H. Abd El-Halim, M. Omar, G. Mohamed, *Spectrochim. Acta A*, 78 (2011) 36-44.

- [6] S. Patil, S. Unki, A. Kulkarni, V. Naik, U. Kamble, P. Badami. *J. Coord. Chem.* 64 (2011) 323-336.
- [7] A. Singh, Y. Kumar, P. Puri, M. Kumar, C. Sharma, *Eur. J. Med. Chem.* 52 (2012) 313-321.
- [8] F. Gaccroli, R. Gazzola, M. Lanfranchi, L. Marchio, G. Metta, M. Pellinghelli, S. Tardito, M. Tegoni, *J. Inorg. Biochem.* 99 (2005) 1573-1584.
- [9] P. Banerjee, O. Pandey, S. Sengupta. *Transition Met. Chem.* 33(2008) 1047-1052.
- [10] G.Gangadhar, P. Avaji, S. Patil, P. Badami. *Eur. J. Med. Chem.* 43 (2008) 2639-49
- [11] A. Demirbas, D. Sahin, N. Demirbas, S. Karaoglu, *Eur. J. Med. Chem.* 44 (2009) 2896-2903.
- [12] A. K. Singh, O.P. Pandey, S.K. Sengupta. *Spectrochim. Acta (A)* 85 (2012) 1-6.
- [13] R. Issa, M. Gaber, N. Al-Wakiel, S. Fathalla, *Chin J. Chem.*, 30 (2012) 547-556.
- [14] Z. Chohan, S. Sumrra, M. Toussoufi, T. Hadda, *Eur. J. Med. Chem.* 45(2010) 2739-2747.
- [15] S. Sumrra, Z.Chohan, *Spectrochim. Acta A*, 98 (2012) 53-61.
- [16] M. Hanif, Z.H. Chohan *Spectrochim. Acta A*, 104 (2013) 468-476
- [17] G.J. Kharadi *Spectrochim. Acta*, 110 (2013) 311-316
- [18] H. Gou-Qiang, H. Li, X. Song-Qiang, H. Wen-Long, *Chin. J. Chem.* 26 (2008) 1145-1149.
- [19] B. S. Holla, B. Veeredra, M. K. Shivanda, B. Poojar, *Eur. J. Med. Chem.*, 38 (2003),759-767.
- [20] J. Hong, Y. Jiao, J. Yan, W. He, Z. Guo, L. Zhu, J. Zhang, *Inorg. Chim. Acta*, 363 (2010) 793-798.
- [21] V. da Silveira, H. Benezra, J. Luz, R. Georg, C. Oliveira, A. Ferreira, *J. Inorg. Biochem.* 105 (2011) 1692-1703.
- [22] M. Saif, Mahmoud M. Mashaly, Mohamed F. Eid, R. Fouad, *Spectrochim. Acta A*, 92 (2012) 347- 356
- [23] P. Kavitha, M. Saritha, K. reddy, *Spectrochim. Acta A*, 102 (2013) 159-168.
- [24] G. Li, K. Du, J. Wang, J. Liang, J. Kou, X. Hou, L. Ji, H. Chao, *J. Inorg. Biochem.* 119 (2013) 43-53.
- [25] M. Shebl, *Spectrochim. Acta A*, 117 (2014) 127-137.

- [26] W. Song , J. Cheng , D. Jiang , L. Guo M. Cai H. Yang Q. Lin ` Spectrochim. Acta A, 121 (2014) 70-76.
- [27] N. Raman, R. Mahalakshmi, L. Mitu, Spectrochim. Acta A, 131 (2014) 355-364
- [28] S. Rubino, P. Portanova, A. Albanese, G. Calvaruso, S. Orecchio, G. Fontana, G.C. Stocco J. Inorg. Biochem., 101 (2007) 1473-1482
- [29] A. I. Matesanz, P. Souza J. Inorg. Biochem, 101 (2007) 245-253
- [30] N. Shahabadi, S. Kashanian, M. purfoulad, Spectrochim. Acta A, 72 (2009) 757-761
- [31] D. Montagner, V. Gandin, C. Marzano, B. Longato, J. Inorg. Biochem. 105 (2011) 919-926.
- [32] E. Ulukaya, F. Ari, K. Dimas, E. Ikitimur, E. Guney, V. Tilmaz, Eur. J. Med. Chem. 46 (2011) 4957-4963.
- [33] N. Abdel Ghani, A. Mansour, Eur. J. Med. Chem. 47 (2012) 399-411
- [34] M. Patel, P. Dosi, B. Bhalt, Spectrochim. Acta A, 86 (2012) 508-514.
- [35] M. El-Shahawi, M. Al-Jahdali, A. Bashammakh, A. Al-Sibaai, H. Nassef, Spectrochim. Acta A 113 (2013) 459-465.
- [36] U. Ozdemir, N. Akkaya, N. Ozbek, Inorg. Chim. Acta, 400 (2013) 13-19.
- [37] N. Ozbek, S. Alyar, H. Alyar, E. Sahin, N. Karacan, Spectrochim. Acta A, 108 (2013) 123-132.
- [38] K. Ibrahim, R. Zaky, E. Gomaa, M. Abd El-Hady, Spectrochim. Acta A, 107 (2013) 133-144.
- [39] M. Dordevic, D. Jeremic, M. Rodic, V. Simic, I. Brceski, V. Leovac, Polyhedron 68 (2014) 234-240.
- [40] A.M. Khedr, M. Gaber, E.H. Abd El-Zaher Chinese J. Chem., 29 (2011).1124-1132.
- [41] M. Gaber, Y.S. El-Sayed , K.Y. El-Baradie, R. M. Fahmy, Spectrochim. Acta, A, 107 (2013) 359-370; N. El-Wakiel, Y. El-Sayed, M. Gaber J. Mol. Struct., 1001 (2011) 1-11.
- [42] M. Gaber, N. A. El-Wakiel, H. El-Ghamry, S. K. Fathalla J. Mol. Struct. 1076 (2014) 251-261
- [43] M.E. Reichmann, C.A. Rice, C.A. Thomos, P. Doty, J. Amer. Chem. Soc. 76 (1954) 3047- 3053.
- [44] J. Marmur, J. Mol. Biol. 3 (1961) 208.
- [45] N. Li, Y. Ma, C. Yang, L. Guo, X. Yang, Biophys. Chem. 116 (2005) 199-205.

- [46] H. P. Aishakhanam, P. B. Raghavendra, N. N. Ganesh, S. F. Christopher, B. G. Kalagouda, *Polyhedron* 34 (2012) 149–156.
- [47] A. Bauer, W. Kirby, C. Sherris, M. Turck, *American Journal of Clinical Pathology*, 45 (1966) 493-496.
- [48] M. Pfaller, L. Burmeister, M.A. Bartlett, and M.G. Rinaldi. *J. Clin. Microbiol.* 26 (1988) 1437-1441.
- [49] P. Skehan, R. Storeng, *J. Natl. Cancer Inst.* 82, (1990) 1107-1112.
- [50] National committee for Clinical laboratory standards, NCCLS approval Standard document M2-A7, Vilanova, PA, 2000.
- [51] A. Ardestani, R. Yazdanparast, *Food Chemistry* 104 (2007) 21–29.
- [52] W. J. Geary, *Coord. Chem. Rev.*, 7 (1971) 81-122.
- [53] N. T. Madhu, P. K. Radhakrishnan, *Trans. Met. Chem.* 25 (2000), 287-292.
- [54] A. Prakash, B. Singh, N. Bhojak, D. Adhikari, *Spectrochim. Acta A*, 76 (2010) 356-362.
- [55] A. Golcu, M. Tumer, H. Demirelli, R. Wheatley, *Inorg. Chim. Acta*, 358 (2005) 1785-1797.
- [56] K. Nakamoto, *Infrared and Raman Spectra of Inorganic and Coordination Compounds*, Wiley-Interscience, New York, 1986.
- [57] D. X. West, A. Nassar, F. A. El-Saied, M. I. Ayad, *Transition Met. Chem.*, 23 (1998) 423-427.
- [58] A. B. Lever, *Inorganic Electronic Spectroscopy*, Elsevier, Amsterdam 1968.
- [59] C. Jorgensen, *Absorption Spectra and Chemical Bonding in Complexes*, Pergamon Press, London (1964).
- [60] A.B. Lever, *Inorganic electronic Spectroscopy*, 2nd Ed. Elsevier Amsterdam 1982, 544-552.
- [61] A. W. Coats, J.P. Redfern, *Nature* 201 (1964) 68-69.
- [62] A. Frost, R. Pearson, *Kinetics and Mechanism*, John Wiley and Sons, New York, 1961.
- [63] U. El-Ayaan, I. Kenawy, Y. Abu El-Reash, *Spectrochim. Acta A*, 68 (2007) 211.
- [64] N. Chitrapriya, V. Mahalingam, M. Zeller, K. Natarajan, *Inorg. Chim. Acta*, 363 (2010) 3685-3693.
- [65] S. Tysoe, R. Morgan, A. Baker, T. Streaks, *J. Phys. Chem.*, 97 (1993) 1707-1711.

- [66] F. Firdaus, K. Fatma, M. Azam, S. Khan, A. Khan, M. Shakir, *Transition Met. Chem.* 33 (2008) 467-473.
- [67] M. Patel, D. Gandhi, P. Parmar, *Spectrochim. Acta, A*, 84 (2011) 243-248.
- [68] R. Vijayalakshmi, M. Kanthimathi, V. Subramanian, B. Nair, *Biochem. Biophys. Acta*, 1475 (2000) 157.
- [69] X. Liu, Z. Chen, L. Li, Y. Chen, J. Lu, D. Zhang, *Spectrochim. Acta A*, 102 (2013) 142-149.
- [70] R. Indumathy, M. Kanthimathi, T. weyhermuller, B. Nair, *Polyhedron* 27 (2008) 3443-3450.
- [71] S. Sathyanarayana, J. dabroniak, J. Chaires, *Biochem.* 31 (1992) 9319-9324.
- [72] L. Jin, P. Yang, *J. Inorg. Biochem.* 68 (1997) 79-83.
- [73] M. Patel, H. Josh, C. Patel, *Spectrochim. Acta A*, 104 (2013) 48-55.
- [74] W.T. Shier, *Mammalian Cell Culture on \$5 a Day: A Lab Manual of Low Cost Methods*. University of the Philippines, Los Banos, 1991, p 64.
- [75] N. Udilova. A. Kozlov, W. Bieber-Schulte, K. Frei, K. Ehrenberger, H. Nohl, *Biochem. Pharm.* 65 (2003) 59.
- [76] P. Sathyadevi, P. Krishnamoorthy, M. Alagesan, K. Thanigaimani, P. Muthiah, N. Dharmaraj, *Polyhedron*, 31 (2012) 294-306

Figures

Fig. 1 The structure of the Schiff base ligand.

Fig. 2 The kinetic parameters

Fig. 3 The structure of the Schiff base metal complexes.

Fig. 4 The absorption spectra of the ligand and its Ni(II), Pd(II) and Pt(II) complexes in the absence and presence of CT-DNA

Fig. 5 Effect of increasing amount of the prepared compounds on the viscosity of CT-DNA ($3 \times 10^{-5} \text{M}$)

Fig. 6 Effect of prepared compounds on HEPG2 cell line

Tables

Table 1: The results of the elemental analyses and the molar conductance values of the metal complexes.

Table 2: The IR spectra of the metal complexes

Table 3: ^1H NMR of the Schiff base ligand, Pd and Pt complexes

Table 4: The thermodynamic parameters (ΔE , ΔH , ΔS and ΔG) of Ni(II), Pd(II) and Pt(II) complexes.

Table 5: The antibacterial and antifungal activity values of the investigated compounds.

Table 6: *In vitro* antitumor activities of prepared compounds against HEPG2 cell line.

Table S1: The stages of decomposition, temperature range, weight loss percentages and decomposition products of the metal complexes.

Table S2: Binding constants ($K_b \text{ M}^{-1}$) of the interaction between the complexes of the Schiff-base and CT-DNA.

Table 1: Elemental analysis and physical properties of the prepared compounds

Compounds	Molecular formula (Empirical formula)	Mol. wt. (m.p.)	Yield %	Elemental analysis Calc / (found)			A_m
				%C	%H	%M	
SB	$C_{13}H_{10}N_4O$	(238) 240	92	65.5 (65.85)	4.2 (4.8)	-	-
C1	$C_{13}H_{13}ClN_4O_3Ni$ [NiLCl.H ₂ O].H ₂ O	367.5 > 300	89	42.45 (42.27)	3.54 (3.91)	16.05 (15.55)	5.98
C2	$(C_{13}H_{15}ClN_4O_4Pd)$ [PdLCl.H ₂ O].2H ₂ O	432.5 > 300	70	36.07 (36.12)	3.47 (3.02)	24.51 (24.03)	8.23
C3	$C_{13}H_{13}ClN_4O_4Pt$ [PtLCl.H ₂ O].H ₂ O	503.5 > 300	72	30.98 (31.37)	2.58 (2.89)	38.73 (38.95)	10.12

SB (Schiff base ligand)

Table 2: IR bands of the prepared compounds

Compounds	ν_{OH}	ν_{NH}	$\nu_{C=N}$ (Traizole)	$\nu_{C=N}$ (Schiff)	ν_{M-O}	ν_{M-N}	ν_{C-O}
	SB	3437	3105	1614	1575	-	-
C1	3378	3126	1617	1538	556	426	1280
C2	3413	3148	1621	1545	600	521	1307
C3	3405	3146	1627	1553	611	535	1313

Table 3: The ¹HNMR spectra of complexes under investigation recorded in d⁶- DMSO at 25 °C.

Compounds	δ_{NH}	$\delta_{HC=N}$	δ_{OH}	$\delta_{aromatic}$
SB	14.16	8.44	10.08	7.17-8.08
C2	10.935	8.93	-	7.27-7.99
C3	10.809	8.95	-	6.74-8.14

Table 4: Temperature of decomposition and activation parameters (ΔH , ΔS , ΔG) for decomposition of complexes

<i>Complex</i>	<i>n</i>	<i>Step</i>	<i>r</i>	<i>T (K)</i>	<i>E</i>	ΔH	<i>A</i>	$-\Delta S$	ΔG
C1	1	1 st	0.9901	360	44.195	41.240	3718.5367	0.186	107.48
	1	2 nd	0.9634	546	13.557	9.169	884107802.4	0.087	54.93
	0	3 rd	0.9827	711	169.055	163.158	0.0789342	0.282	362.84
	0.33	4 th	0.9998	773	158.592	152.082	4.190	0.249	347.31
	1	5 th	0.9980	869	128.117	121.013	2097.69	0.198	290.53
C2	1	1 st	0.9963	345.5	53.635	50.758	79.714	0.218	126.21
	1	2 nd	0.9986	541.5	35.742	30.966	8569596.37	0.126	103.33
	1	3 rd	0.9732	670.5	46.057	40.443	4291349.97	0.133	130.28
	1	1 st	0.9946	364.5	55.349	52.487	49.203	0.222	128.92
C3	0.66	2 nd	0.9999	671	104.767	98.634	2538.11	0.196	242.92

E: the activation energy ($\text{KJ}\cdot\text{mol}^{-1}$), ΔH : the activation enthalpy ($\text{KJ}\cdot\text{mol}^{-1}$), ΔS : the entropy ($\text{J}\cdot\text{K}^{-1}\cdot\text{mol}^{-1}$), A: the pre-exponential factor (s^{-1}), ΔG : the free energy ($\text{KJ}\cdot\text{mol}^{-1}$).

Table 5: The antibacterial and antifungal activity values of the investigated compounds

<i>Compound</i>	<i>Inhibition zone diameter (mm / mg sample)</i>			
	<i>Escherichia coli</i> (G-)	<i>Staphylococcus aureus</i> (G+)	<i>Aspergillus flavus</i> (fungus)	<i>Candida albicans</i> (fungus)
SB	10	13	0	11
C1	9	10	0	9
C2	11	13	0	9
C3	10	12	0	9
Tetracycline Antibacterial agent	31	29	-	-
Amphotericin B Antifungal agent	-	-	16	19

Table 6: *In vitro* antitumor activities of prepared compounds against HEPG2 cell line

<i>Compound</i>	<i>IC₅₀ (μg/mL)</i> <i>(HEPG2)</i>
SB	4.3
C1	15.5
C2	19.7
C3	19.5
Dox.	4

Dox: doxorubicin, standard cytotoxin drug

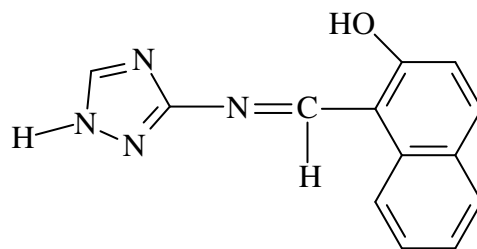


Fig.1. The structure of Schiff base ligand, [(1*H*-1,2,4-triazole-3-ylimino)methyl]naphthalene-2-ol

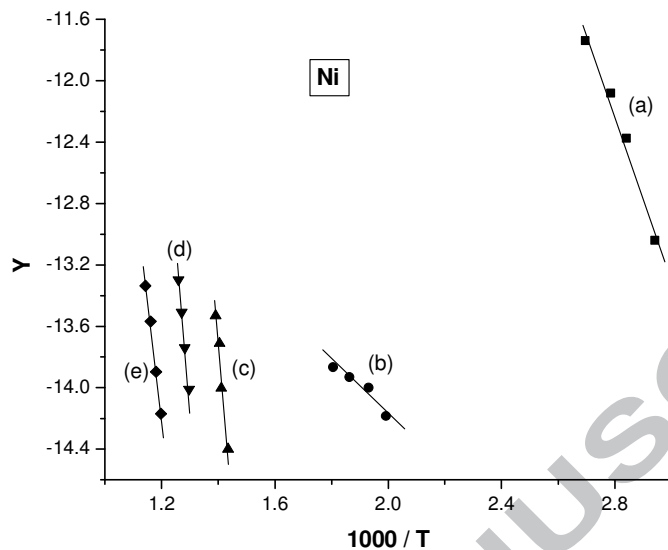


Fig. 2a. Coats-Redfern plot for complex 1.

a) first step b) second step c) third step d) fourth step e) fifth step
 where, $Y = [1 - (1 - \alpha)^{1-n}] / (1-n) T^2$ for $n \neq 1$ or $Y = [-\ln(1 - \alpha)] / T^2$ for $n = 1$

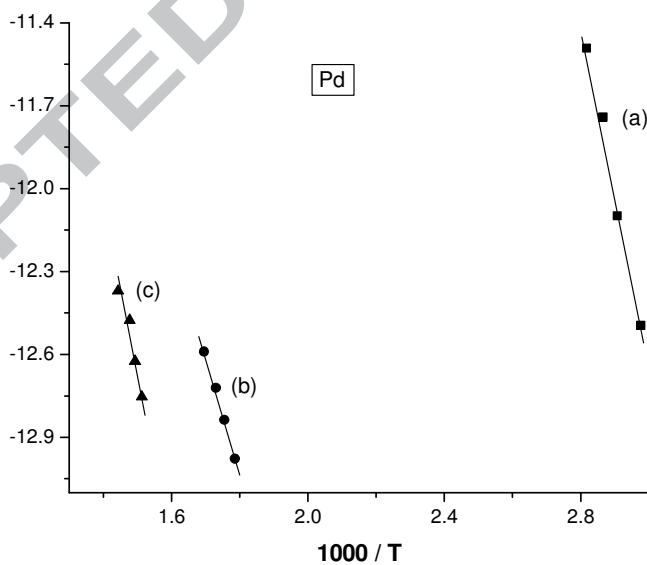


Fig. b. Coats-Redfern plot for complex 2.

a) first step b) second step c) third step
 where, $Y = [1 - (1 - \alpha)^{1-n}] / (1-n) T^2$ for $n \neq 1$ or $Y = [-\ln(1 - \alpha)] / T^2$ for $n = 1$

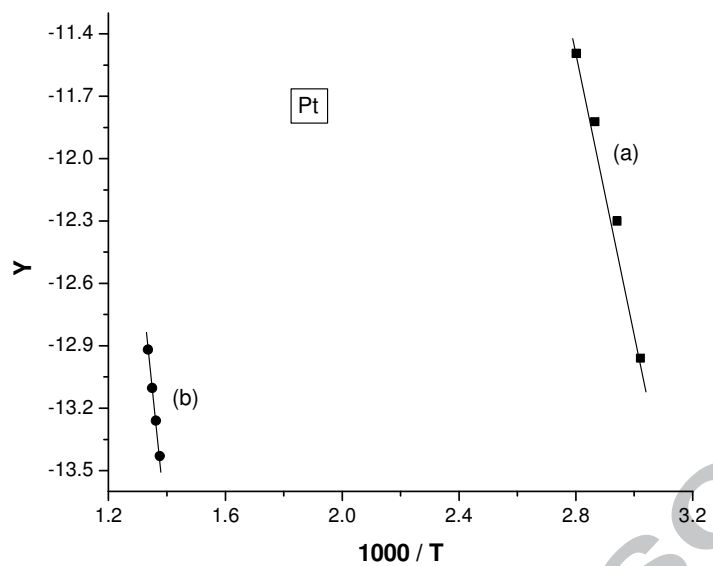


Fig. 2c. Coats-Redfern plot for complex 3.

a) first step b) second step

where, $Y = [1 - (1 - \alpha)^{1-n}] / (1-n) T^2$ for $n \neq 1$ or $Y = [-\ln(1 - \alpha)] / T^2$ for $n = 1$

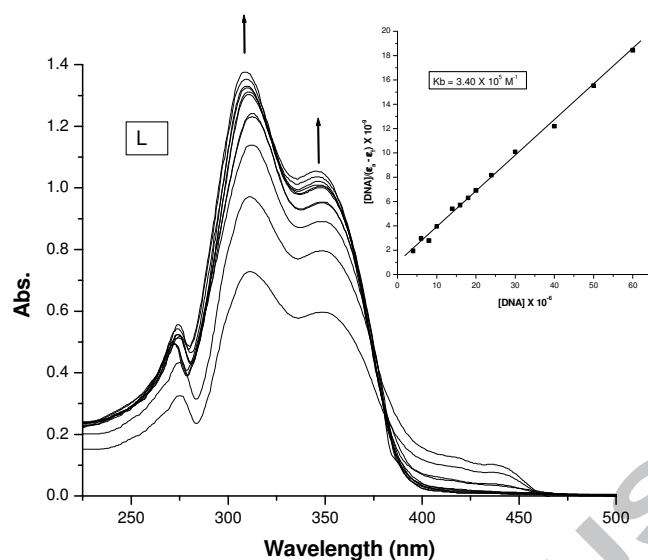


Fig. 4a. Electronic absorption spectra of the ligand in the absence and presence of increasing amounts of CT DNA. Arrows show the changes in absorbance with respect to an increase in the DNA concentration (Inset: Plot of $[DNA]$ vs $[DNA]/(\epsilon_a - \epsilon_f)$. (at **318 nm** $K_b = 3.40 \times 10^5 \text{ M}^{-1}$)

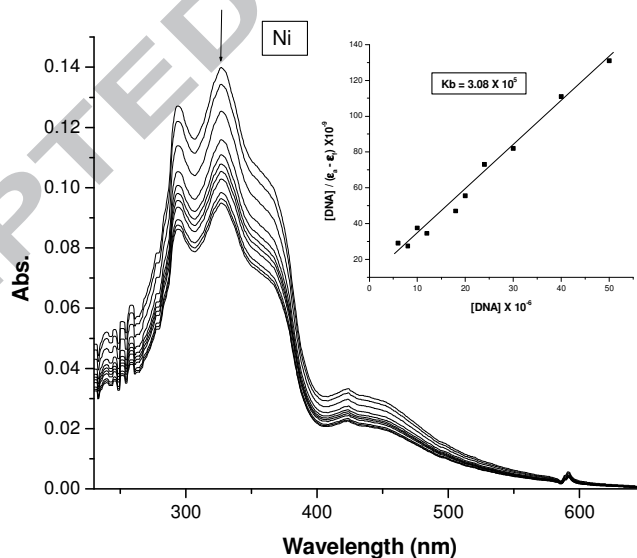


Fig. 4b. Electronic absorption spectra of Ni complex in the absence and presence of increasing amounts of CT DNA. Arrows show the changes in absorbance with respect to an increase in the DNA concentration (Inset: Plot of $[DNA]$ vs $[DNA]/(\epsilon_a - \epsilon_f)$. (at **319 nm** $K_b = 3.08 \times 10^5 \text{ M}^{-1}$)

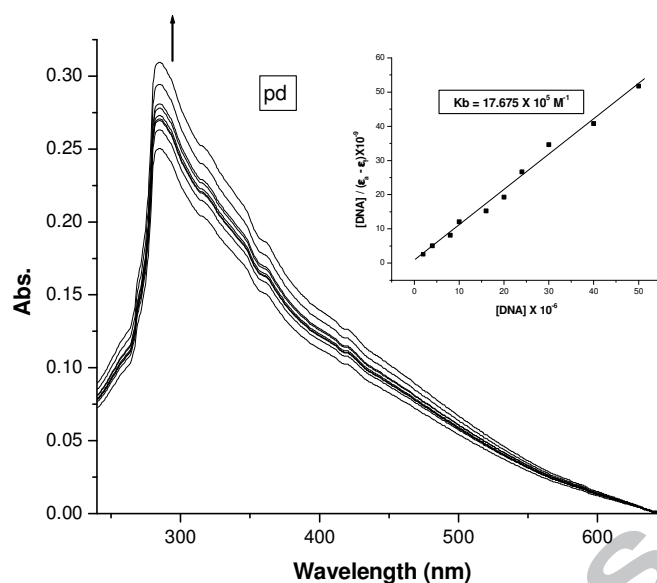


Fig. 4c. Electronic absorption spectra of Pd complex in the absence and presence of increasing amounts of CT DNA. Arrows show the changes in absorbance with respect to an increase in the DNA concentration (Inset: Plot of $[DNA]$ vs $[DNA]/(\epsilon_a - \epsilon_f)$. (at **288 nm** $K_b = 17.675 \times 10^5 \text{ M}^{-1}$)

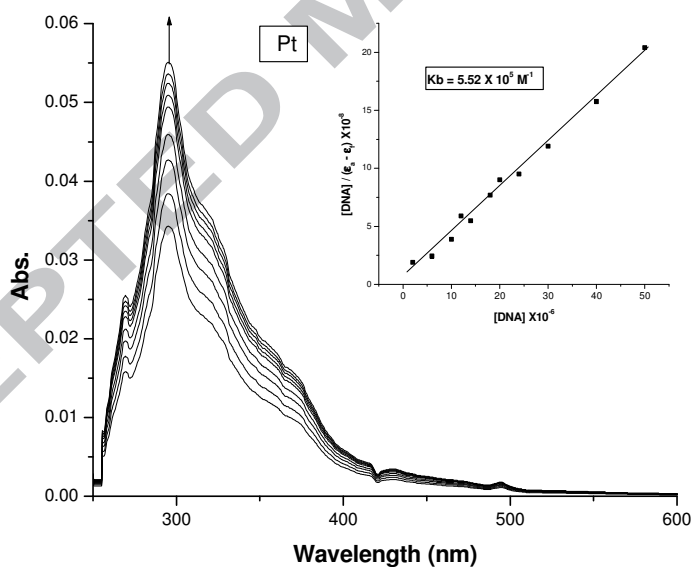


Fig. 4d. Electronic absorption spectra of Pt complex in the absence and presence of increasing amounts of CT DNA. Arrows show the changes in absorbance with respect to an increase in the DNA concentration (Inset: Plot of $[DNA]$ vs $[DNA]/(\epsilon_a - \epsilon_f)$. (at **320 nm** $K_b = 5.52 \times 10^5 \text{ M}^{-1}$)

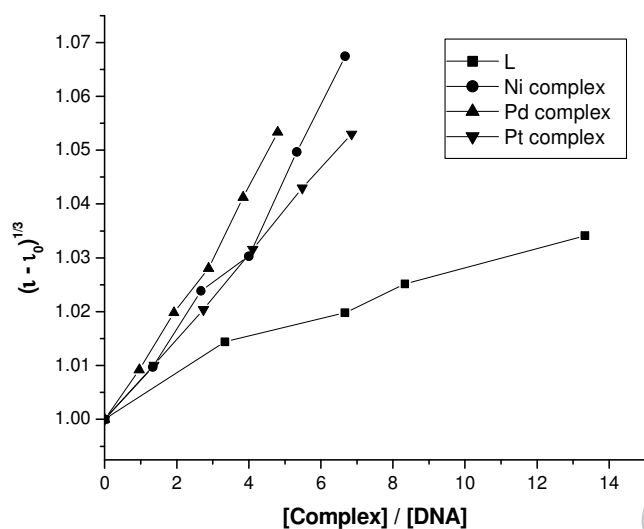


Fig. 5. Effect of increasing amount of the prepared compounds on the viscosity of CT-DNA ($3 \times 10^{-5} \text{M}$)

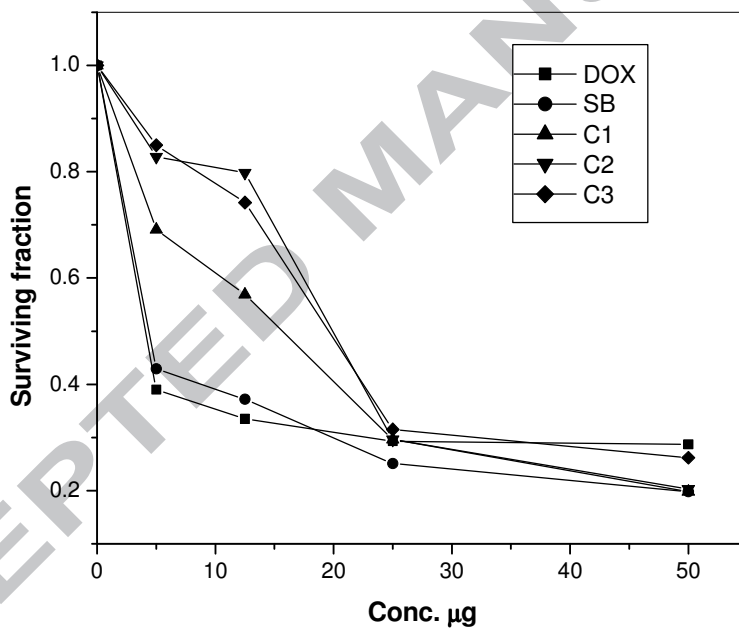
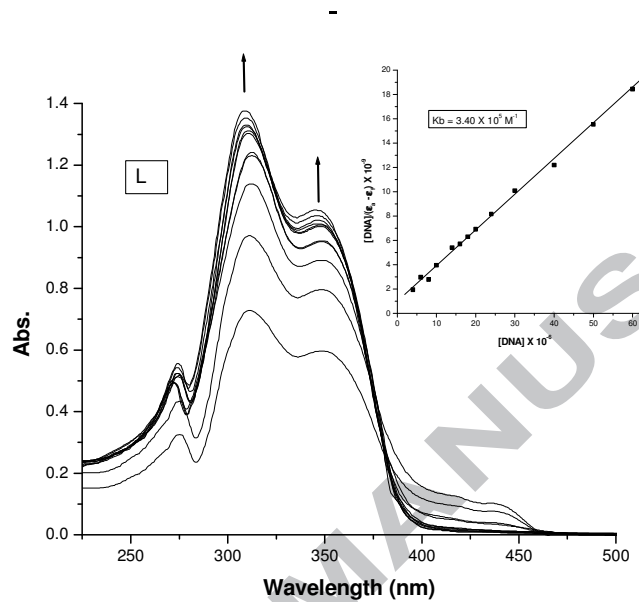


Fig. 6. Effect of prepared compounds on HEPG2 cell line

Ni(II), Pd(II) and Pt(II) complexes of (1*H*-1,2,4-triazole-3-ylimino)methyl]naphthalene-2-ol. Structural, spectroscopic, biological, cytotoxicity and DNA binding.



- Ni(II), Pd(II) and Pt(II) Schiff base complexes
- Pd(II) and Pt(II) Square planar complexes and tetrahedral Ni(II) complex.
- The biological, antioxidant and anticancer activity
- The DNA-binding properties of the complexes.

ACCEPTED MANUSCRIPT